

A Comparative Study of Structural Representations for 2D Materials: Insights from Dynamic Collision Fingerprint and Matminer

Raphael M. Tromer

Institute of Physics, University of Brasília, 70910-900 Brasília, Federal District, Brazil

Isaac M. Felix

*Center for Agri-food Science and Technology, Federal University of Campina Grande,
58840-000 Pombal, Paraíba, Brazil*

Rafael Besse

*International Center of Physics, Institute of Physics, University of Brasília, 70910-900
Brasília, Federal District, Brazil*

Marcelo L. Pereira Junior

*Department of Electrical Engineering, College of Technology, University of Brasília,
70910-900 Brasília, Federal District, Brazil*

Marcos G. E. da Luz

*Department of Physics and Multidisciplinary Laboratory for Modeling and Analysis of
Data in Complex Systems (MADComplex), Center for Scientific Modeling and
Computing, Federal University of Paraná, 81531-980 Curitiba, Paraná, Brazil*

Abstract

In materials science, the selection of structural descriptors for machine learning protocols strongly influences predictive performance and the degree of physical interpretability that can be achieved from the derived models. Although more complex descriptors may improve numerical accuracy, they often represent extra computational load, also reducing transparency into the underlying structural information. A framework called the Dynamic Collision Fingerprint (DCF) was recently proposed with the goal of producing concise, physically significant representations, generating descriptors via dy-

namical probing of atomic structures. In this work, we benchmark DCF using a dataset composed of 120 two-dimensional carbon allotropes and compare its performance with the widely considered Matminer library. The analysis employs three regression models, linear regression, decision tree, and XGBoost, evaluated over train and test partitions ranging from 10% to 90% and repeated over multiple random seeds in order to characterize statistical variability. The obtained results demonstrate that DCF easily matches Matminer in terms of predicting accuracy across all learning algorithms. However, it accomplishes this using descriptors that are significantly lower dimensional, pointing to manageable computing costs. Moreover, compared to the rather technical Matminer descriptions, the DCF exhibits considerably clearer physical interpretability. These findings suggest that DCF is a significant substitute for high-dimensional descriptor libraries as structural representation since it is both computationally flexible and physically grounded.

Keywords: Dynamic Collision Fingerprint, Matminer, Machine Learning Descriptors, Two-dimensional Carbon Allotropes

1. Introduction

Atomic level structural characterization constitutes a central element of materials science and computational chemistry, since it provides the basis for establishing structure property relationships that guide both experimental interpretation and the rational design of novel materials [1, 2, 3, 4, 5, 6, 7, 8, 9]. Over the last decade, the integration of atomistic simulations, structural descriptors, and machine learning models has significantly transformed high throughput materials discovery [8, 9, 10, 11, 12, 13]. In this context, the definition of descriptors that are simultaneously efficient, interpretable, and transferable has emerged as a critical challenge, since the predictive capability and robustness of machine learning models depend strongly on the quality and representational adequacy of the selected structural features [14, 15, 16].

A large variety of structural descriptors has been proposed and consolidated in the literature [17, 18, 19, 20, 21, 22, 23, 24]. These approaches include representations based on radial and angular distribution functions, orientational order parameters, spectral formulations such as the Smooth Overlap of Atomic Positionsv (SOAP) method [17], and graph based or topology driven embeddings derived from message passing frameworks [24, 25]. Many of these descriptors are available through dedicated software libraries, among

which Matminer [26] has become widely adopted in computational materials modeling due to its extensive collection of structural, electronic, and chemical features and its support for reproducible workflows across diverse material classes.

Despite such versatility, the employment of generic high-dimensional descriptor libraries often introduces practical limitations when applied to structurally complex systems, the case of two-dimensional (2D) materials. A first limitation concerns the physical interpretability of many features, as they cannot be directly associated with intuitive structural characteristics. A second limitation concerns sensitivity to disorder, defects, and aperiodicity, which are frequently present in 2D systems, where local distortions, vacancies, and topological irregularities are common [27, 28, 29, 30].

Motivated by these challenges, a recently proposed descriptor scheme, the Dynamic Collision Fingerprint (DCF), was introduced aiming to be a more physically based alternative [31]. Guided by well-established concepts from classical statistical mechanics [32, 33], DCF departs from static coordinate-based representations. Instead, it seeks to dynamically probe atomic structures through trajectories of idealized particles undergoing elastic collisions with the lattice. In this way, statistical analyses of free paths, collision angles, recurrence events, and angular symmetries obtained through Fourier analysis and Shannon entropy allow the descriptor to encode structural signatures associated with symmetry, porosity, and disorder [31]. This construction yields descriptors that are directly interpretable in physical terms, independent of electronic or energetic models, and computationally adjustable according to the assumed sampling parameters.

Notwithstanding the promising performance of DCF displayed in its initial work [31], a thorough evaluation against popular high-dimensional descriptor libraries and under controlled and statistically consistent benchmarking settings is still missing. In this contribution we fulfill this gap by systematically contrasting the DCF with the Matminer descriptor library. Using a dataset composed of 120 distinct 2D carbon allotropes, descriptors generated by both approaches are considered within three representative machine learning models, namely, linear regression [34], decision trees [35], and XGBoost [36]. Also, a wide variety of train and test partitions are examined in the comparisons.

The comprehensive analyses carried out in the present work allows to evaluate the DCF’s relative performance in terms of physical interpretability, computing efficiency, prediction accuracy, and resilience. The obtained

results clearly demonstrate that the DCF can be a complementary or even a substitute alternative descriptor scheme for materials informatics workflows. In particular, by reframing structural characterization as a dynamical response problem rather than a purely static geometric picture, we unveil that predictors can be fairly compact (low-dimensional), while retaining the information needed to accurately describe important aspects of 2D materials.

2. Methodology

The methodology followed here comprises dataset preparation, descriptor construction, machine learning modeling, and statistical evaluation, all performed under consistently specified conditions to ensure direct comparability between descriptor approaches. A schematic overview of the complete workflow adopted in this study is presented in Figure 1, summarizing the main stages from dataset preparation to descriptor generation, model training, and statistical validation.

The benchmark dataset employed in this study comprises 120 distinct 2D carbon allotropes originally reported in literature [37]. All coordinates and lattice information for the addressed structures are provided in the Supporting Information (SI). The systems were standardized using the Pymatgen library [38]. Each structure was reduced to its primitive cell, assuming a symmetry tolerance of 10^{-3} Å, and atomic coordinates were scaled to ensure uniform density normalization. The chosen target property is the formation energy reported in the literature [37]. Then, supercells of at least $2 \times 2 \times 1$ are required for appropriate simulations, and this was consistently adopted throughout the study [31].

Two descriptor frameworks were considered, DCF and the Matminer feature library. The DCF model is explained in detail in [31], but its essential points can be summarized as follows. One considers the propagation of classical point particles undergoing elastic collisions within an atomic lattice supercell under periodic boundary conditions. Each trajectory propagates during a specific number of steps N_S . A single “step” corresponds to a straight line segment between successive boundary crossings. For proper averages, a total of N_L trajectories are launched. Along propagation, quantities such as traveled distances and angular deflections are recorded. The final descriptor vector is constructed from statistical analyses of angular distributions using Shannon entropy as well as Fourier decomposition of recurrence frequencies

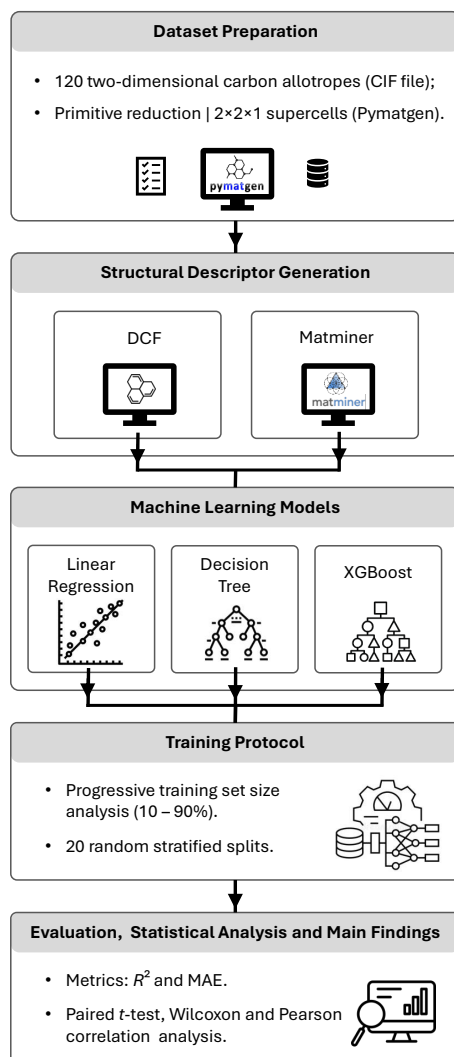


Figure 1: Schematic workflow of the computational pipeline employed in this study. After dataset preparation, structural descriptors were generated using DCF and Matminer, and the models were trained using linear regression, decision trees, and XGBoost. Performance was assessed through MAE and R^2 , complemented by paired statistical tests and correlation analyses.

(associated with one-to-nine-fold lattice symmetries), mean free paths, and recurrence times, with explicit expressions provided in [31].

Unless otherwise explicitly stated, the standard parameterization was $N_S = 10^4$ and $N_L = 200$, yielding descriptor vectors from 25 to 30 dimensions.

Larger N_S and N_L were considered for sensitivity analysis, with the fast (extended) configuration corresponding to $N_S = 10^3$ and $N_L = 100$ ($N_S = 10^4$ and $N_L = 300$). The implementation relies on NumPy, SciPy, and pandas and is available in the repository indicated in this work.

Matminer descriptors were generated from the Matminer library [26]. The descriptor set includes radial distribution functions, binned up to 20 Å and with a resolution of 0.1 Å, packing density and volume per atom statistics, and basic stoichiometric attributes. Depending on the adopted radial distribution function discretization, the resulting feature vectors contain approximately 200-500 components, thus substantially larger than those of DCF. All descriptors were normalized using z score scaling prior to training.

Three representative regression algorithms were addressed. Linear regression was implemented using ordinary least squares from scikit learn. The decision tree model was trained with a maximum depth of 8 and a minimum sample count per leaf of 2. The XGBoost model was implemented with the hyperparameters `n_estimators`, `max_depth`, `learning_rate`, and `subsample` set to 500, 8, 0.05, and 0.8, respectively. Prior to training, all features were standardized to a mean of 0 and a variance of 1. No feature selection or dimensionality reduction was applied in order to preserve direct comparability between descriptor schemes. Fixed hyperparameters were adopted for all models, as the objective here is to compare descriptor families under identical modeling conditions rather than to optimize individual performance.

Predictive robustness was assessed through repeated random train and test partitions, where the test fraction X_T denotes the portion of the dataset assigned to the test set. We considered X_T values ranging from 0.1 to 0.9 in increments of 0.1. Each partition was repeated 20 times with random seeds to ensure statistical reliability, and reported quantities correspond to averages across all seeds.

Predictive performance was quantified using the coefficient of determination R^2 and the mean absolute error (MAE), where MAE corresponds to the average absolute difference between predicted and reference values. To evaluate whether DCF and Matminer exhibit statistically distinguishable performance and to quantify their concordance across test fractions, paired t tests, Wilcoxon signed rank tests, and Pearson correlation analyses were performed on the resulting metric distributions. Statistical analyses were carried out using SciPy, adopting a significance threshold of $p < 0.05$.

3. Results and Discussion

The predictive performance of DCF descriptors was first evaluated with respect to the simulation parameters controlling trajectory sampling. Figure 2 summarizes the dependence of the MAE on X_T for different combinations of N_S and N_L and for the three machine learning models considered in this work.

Across all models, the MAE remains stable with respect to variations in N_S and N_L . As observed in Figure 2(a), the only noticeable deviation corresponds to a single outlier near $X_T \approx 0.8$ in the linear regression case. In contrast, Figure 2(b) and Figure 2(c) show tightly grouped results across the full range of X_T , with differences comparable to the expected statistical fluctuations from random train test partitions. This behavior indicates that the DCF descriptors are robust with respect to moderate variations in trajectory length and sampling density, and that convergence is achieved without the need for extensive parameter tuning.

This stability aligns with the central concept of the DCF formulation [31]: structural information should be better captured through aggregated dynamical statistics rather than through static high-dimensional signatures. Once the trajectory sampling explores the relevant structural motifs, the resulting descriptors become statistically stable. In the present dataset, increasing N_L beyond 100 does not produce systematic gains in predictive accuracy, indicating that relatively inexpensive parameterizations are already sufficient to capture the dominant structural information required for machine learning predictions.

For the following analyzes, we set $N_S = 10^4$ and $N_L = 200$, representing a balanced trade-off between statistical stability and computational cost. Figure 3 compares the predictive performance obtained with DCF and Matminer descriptors through the MAE as a function of X_T for our three machine learning models. The results illustrate that DCF systematically reaches predictive errors comparable to those obtained with Matminer, despite its substantially lower dimensionality and simpler construction.

For linear regression, depicted in Figure 3(a), DCF frequently produces similar or slightly smaller MAE values across several test fractions, with more pronounced differences emerging at larger X_T , where the reduced amount of training data amplifies sensitivity to descriptor quality. In this regime, both approaches occasionally exhibit larger fluctuations, which is expected given the limited expressive capacity of linear models for complex structure

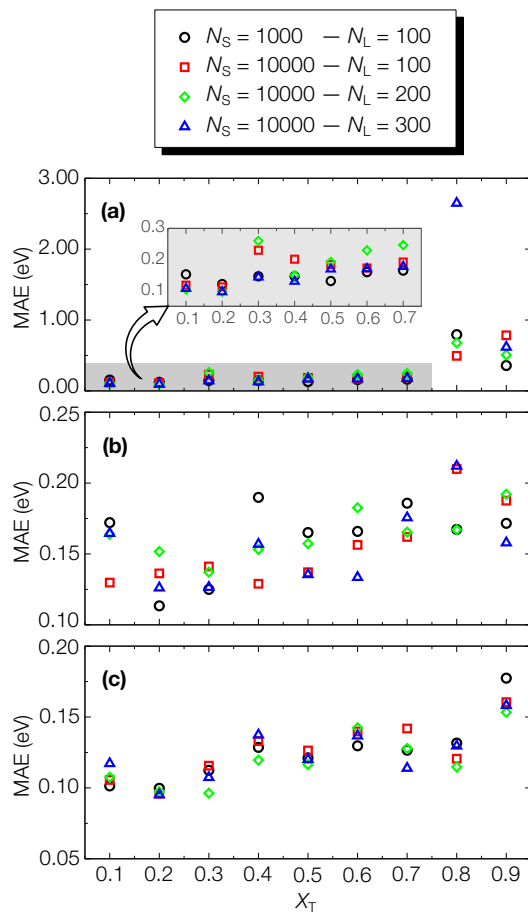


Figure 2: MAE as a function of X_T for different DCF parameterizations defined by N_S and N_L for (a) linear regression, (b) decision tree, and (c) XGBoost.

property relationships. For decision trees, Figure 3(b) shows that the two descriptor frameworks lead to closely overlapping MAE values across most test fractions. Also, both representations provide similar levels of structural information for moderate nonlinear learning.

The comparison becomes even more consistent for XGBoost, as seen from Figure 3(c), which reveals nearly indistinguishable results between DCF and Matminer over the entire range of X_T . This indicates that the essential predictive information captured by the higher-dimensional Matminer representation is effectively retained within the compact DCF when coupled to a strong nonlinear learner.

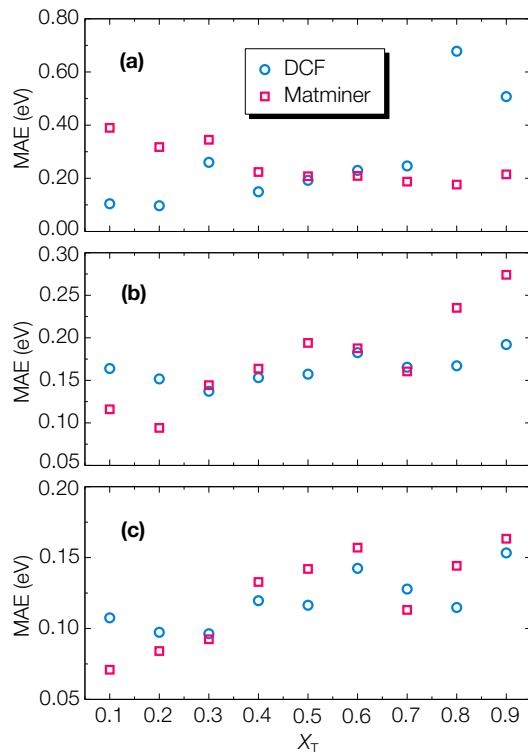


Figure 3: MAE as a function of X_T comparing DCF and Matminer descriptors for (a) linear regression, (b) decision tree, and (c) XGBoost.

An additional perspective on the predictive capability discussed above is obtained by analyzing the coefficient of determination, whose evolution with X_T is shown in Figure 4 for DCF and Matminer descriptors. We recall that while MAE quantifies the absolute prediction error, R^2 provides additional insight into how effectively each descriptor framework captures the variance of the target property across different train and test partitions.

In the linear regression case, Figure 4(a), both descriptor sets lead to low predictive power, with R^2 values fluctuating around zero and occasionally becoming negative at larger X_T . This trait is consistent with the limited flexibility of linear models when applied to complex, intrinsically nonlinear structure-property relationships, reinforcing the interpretation already suggested by the MAE analysis. The decision tree model, Figure 4(b), indicates a clear gain in predictive power, with predominantly positive R^2 values across the tested splits. The agreement between DCF and Matminer remains strong,

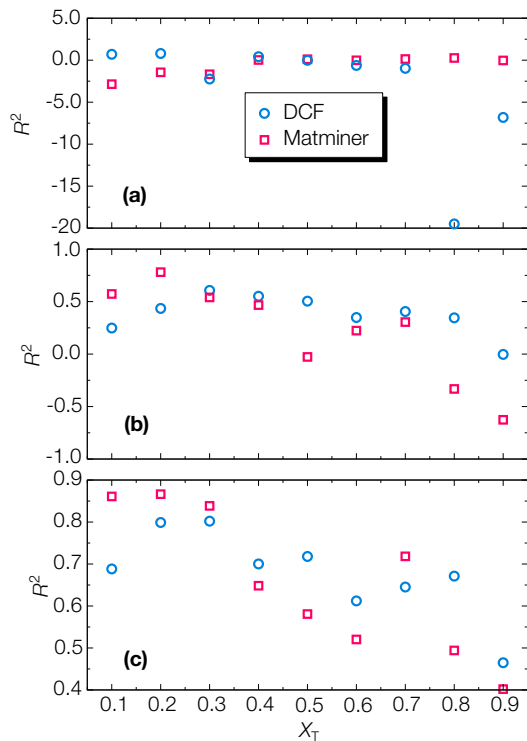


Figure 4: R^2 as a function of X_T comparing DCF and Matminer descriptors for (a) linear regression, (b) decision tree, and (c) XGBoost.

for the small differences observed in specific regions of X_T not altering the overall picture of comparable performance.

The aforementioned agreement becomes even stronger for XGBoost, Figure 4(c). Indeed, the plots show consistently high R^2 values for both descriptor frameworks. The close overlap between the results confirms that DCF captures essentially the same predictive information content as Matminer when combined with a sufficiently expressive nonlinear learner. Variations between individual points remain within the range expected from statistical fluctuations across different random train-test partitions.

Beyond just the crude face value of predictive metrics, it is also relevant to examine how the two descriptor protocols differ in terms of dimensionality, interpretability, and computational cost, as these aspects directly affect their practical applicability in large-scale materials informatics workflows. A central distinction concerns feature dimensionality and physical transparency. The DCF representation remains compact, typically contain-

Table 1: **Comparison between DCF and Matminer in terms of feature dimensionality, interpretability, computational cost per structure, and overall predictive behavior.** DCF standard corresponds to $N_S = 10^4$ and $N_L = 200$, while DCF fast corresponds to $N_S = 10^3$ and $N_L = 100$. Performance summaries are consistent with the trends discussed from Figures 3 and 4. For the Matminer descriptor set, the dimensionality range depends on the selected presets, including RDF binning range and resolution, as well as optional feature subsets.

Descriptor set	#Features	Interpretability	Time per structure	Performance summary
DCF (Standard)	~25-30	High (physics based)	~4 min	Predictive accuracy comparable to Matminer for both MAE and R^2 , with consistent performance for decision tree and XGBoost models.
DCF (Fast)	~25-30	High (physics based)	~30 s	Results remain very close to the standard configuration, with differences within the statistical variations observed in Fig. 2.
Matminer	~200-500	Moderate to low (bin based)	~10 s	Comparable MAE and R^2 behavior relative to DCF, showing similar trends for decision tree and XGBoost models.

ing approximately 25 to 30 descriptors, each one directly associated with a physical or geometric characteristic, as the already mentioned mean free path, recurrence time, angular entropy, and rotational symmetry intensities from 1 to 9-fold. In contrast, the Matminer representation contains several hundred features, largely derived from discretizing the radial distribution function across multiple distance bins (up to approximately 20 Å), complemented by density and packing statistics. While such a high-dimensional description is versatile and broadly applicable, individual components are less intuitive from a physical perspective; note that isolated RDF bins rarely carry a clear standalone interpretation.

A second relevant aspect concerns computational cost. In the current workflow, Matminer requires approximately 10 s per structure, whereas DCF in its standard configuration ($N_S = 10^4$, $N_L = 200$) requires approximately 4 min per structure. However, the stability analysis previously discussed shows that the DCF’s performance is only weakly sensitive to the trajectory-sampling parameters. Even the fast configuration ($N_S = 10^3$, $N_L = 100$) yields MAE values very close to those obtained with more extensive sampling, while reducing the average wall time to roughly 30 s per structure. In this regime, the necessary computational work is fairly of the same order than that of Matminer, while maintaining comparable predictive accuracy across

most training and test partitions.

Taken together with the results shown in Figures 3 and 4, these observations highlight a clear trade-off between descriptor compactness, interpretability, and computational efficiency. Linear models remain limited across both descriptor frameworks, whereas decision tree and XGBoost models consistently achieve high predictive performance, demonstrating that DCF preserves the essential structural information despite its reduced dimensionality. A consolidated comparison summarizing dimensionality, interpretability, computational cost, and predictive behavior is presented in Table 1.

To further complement the performance trends discussed above, additional statistical analyses were conducted to evaluate whether DCF and Matminer exhibit significant differences across the full ensemble of repeated random splits. Paired statistical tests were applied to the metric distributions obtained from 20 random seeds for each X_T value, along with correlation analyses across test fractions. This provides a quantitative assessment of agreement between descriptor frameworks beyond direct visual comparison.

For linear regression, no statistically significant differences were detected between DCF and Matminer for either R^2 or MAE. Both paired t -tests and Wilcoxon signed-rank tests yielded non-significant outcomes ($p > 0.05$), indicating that the small variations observed between descriptors are compatible with statistical fluctuations rather than systematic performance differences. Correlation analyses across test fractions revealed weaker alignment than in nonlinear models, consistent with the higher variability observed in this regime, particularly at large X_T 's, when both descriptor sets can produce unstable, even negative, R^2 values. For the decision tree model, paired statistical tests again indicated no relevant distinctions between DCF and Matminer for either MAE or R^2 ($p > 0.05$). Also, performance trends across test fractions remain positively correlated, pointing to similar responses of both descriptor frameworks to variations in training-set size. Regimes where performance improves or degrades, therefore, tend to coincide for DCF and Matminer, corroborating the traits observed in Figures 3(b) and 4(b). For XGBoost, paired t -tests and Wilcoxon tests show that DCF and Matminer are statistically indistinguishable across all evaluated metrics ($p > 0.05$), while correlation analyses across test fractions reveal strongly positive alignment for both MAE and R^2 .

4. Conclusions

This work presented a systematic comparison of the DCF and Matminer descriptor frameworks, evaluating their predictive performance across multiple machine learning models and train–test data splits. The analysis combined direct performance curves, statistical tests, and an explicit comparison of descriptor dimensionality, interpretability, and computational cost.

Across the full set of simulations, both descriptors exhibited similar predictive limits under linear regression, in which model simplicity dominates the learning behavior and leads to unstable performance at large test fractions. In contrast, nonlinear learners consistently displayed higher accuracy, as it should be expected given the dataset inherently nonlinear structure–property relationships. Actually, for decision tree and XGBoost models, DCF and Matminer converged to closely aligned performance profiles. Statistical tests confirmed the absence of significant differences between the two descriptor sets, while correlation analyses across test fractions revealed consistent predictive trends.

More generally, the present contribution comprehensively illustrated a key trade-off between descriptor compactness, interpretability, and computational efficiency. On one hand, Matminer offers a broad, computationally efficient representation but relies on a high-dimensional feature space that is often less directly interpretable. On the other hand, DCF provides a physically grounded and compact descriptor whose components remain closely associated with structural and dynamical characteristics, while still achieving competitive predictive performance. Furthermore, the stability of DCF under reduced sampling parameters enables substantial reductions in computational cost without significant loss of accuracy, reinforcing its practical usefulness. These positive features support the use of DCF as an effective and scalable framework for data-driven investigations of structure–property relationships in complex materials systems.

Conflicts of interest

There are no conflicts to declare.

Acknowledgements

This work was supported by the National Council for Scientific and Technological Development (CNPq), the Coordination for the Improvement of

Higher Education Personnel (CAPES), and the Federal District Research Support Foundation (FAPDF). RMT acknowledges CNPq for financial support (grant no. 307371/2025-5). MLPJ acknowledges financial support from FAPDF (grant no. 00193-00001807/2023-16), CNPq (grants no. 444921/2024-9 and 308222/2025-3), and CAPES (grant no. 88887.005164/2024-00). MGEL acknowledges financial support from CNPq (grants no. 307512/2023-1 and 04577/2021-0) and CAPES (grant no. 88881.311780/2018-00).

References

- [1] L. M. Ghiringhelli, J. Vybiral, S. V. Levchenko, C. Draxl, M. Scheffler, Big data of materials science: critical role of the descriptor, *Phys. Rev. Lett.* 114 (10) (2015) 105503. doi:<https://doi.org/10.1103/PhysRevLett.114.105503>. URL <https://doi.org/10.1103/PhysRevLett.114.105503>
- [2] A. Ludwig, Discovery of new materials using combinatorial synthesis and high-throughput characterization of thin-film materials libraries combined with computational methods, *npj Comput. Mater.* 5 (1) (2019) 70. doi:<https://doi.org/10.1038/s41524-019-0205-0>. URL <https://doi.org/10.1038/s41524-019-0205-0>
- [3] P. M. Maffettone, L. Banko, P. Cui, Y. Lysogorskiy, M. A. Little, D. Olds, A. Ludwig, A. I. Cooper, Crystallography companion agent for high-throughput materials discovery, *Nat. Comput. Sci.* 1 (4) (2021) 290–297. doi:<https://doi.org/10.1038/s43588-021-00059-2>. URL <https://doi.org/10.1038/s43588-021-00059-2>
- [4] J. Ma, B. Cao, S. Dong, Y. Tian, M. Wang, J. Xiong, S. Sun, MLMD: a programming-free AI platform to predict and design materials, *npj Comput. Mater.* 10 (1) (2024) 59. doi:<https://doi.org/10.1038/s41524-024-01243-4>. URL <https://doi.org/10.1038/s41524-024-01243-4>
- [5] K. Shahzad, A. I. Mardare, A. W. Hassel, Accelerating materials discovery: combinatorial synthesis, high-throughput characterization, and computational advances, *Sci. technol. Adv. Mater.: Meth.* 4 (1) (2024) 2292486. doi:<https://doi.org/10.1080/27660400.2023.2292486>. URL <https://doi.org/10.1080/27660400.2023.2292486>

- [6] K. Song, A. N. M. Tanvir, M. O. Bappy, Y. Zhang, New directions for thermoelectrics: A roadmap from high-throughput materials discovery to advanced device manufacturing, *Small Sci.* 5 (3) (2025) 2300359. doi:<https://doi.org/10.1002/smsc.202300359>. URL <https://doi.org/10.1002/smsc.202300359>
- [7] C. Zeni, R. Pinsler, D. Zügner, A. Fowler, M. Horton, X. Fu, Z. Wang, A. Shysheya, J. Crabbé, S. Ueda, et al., A generative model for inorganic materials design, *Nature* 639 (8055) (2025) 624–632. doi:<https://doi.org/10.1038/s41586-025-08628-5>. URL <https://doi.org/10.1038/s41586-025-08628-5>
- [8] A. E. Allen, A. Tkatchenko, Machine learning of material properties: Predictive and interpretable multilinear models, *Sci. Adv.* 8 (18) (2022) eabm7185. doi:<https://doi.org/10.1126/sciadv.abm7185>. URL <https://doi.org/10.1126/sciadv.abm7185>
- [9] A. Merchant, S. Batzner, S. S. Schoenholz, M. Aykol, G. Cheon, E. D. Cubuk, Scaling deep learning for materials discovery, *Nature* 624 (7990) (2023) 80–85. doi:<https://doi.org/10.1038/s41586-023-06735-9>. URL <https://doi.org/10.1038/s41586-023-06735-9>
- [10] A. Jain, Y. Shin, K. A. Persson, Computational predictions of energy materials using density functional theory, *Nat. Rev. Mater.* 1 (1) (2016) 1–13. doi:<https://doi.org/10.1038/natrevmats.2015.4>. URL <https://doi.org/10.1038/natrevmats.2015.4>
- [11] K. Kim, L. Ward, J. He, A. Krishna, A. Agrawal, C. Wolverton, Machine-learning-accelerated high-throughput materials screening: Discovery of novel quaternary heusler compounds, *Phys. Rev. Mater.* 2 (12) (2018) 123801. doi:<https://doi.org/10.1103/PhysRevMaterials.2.123801>. URL <https://doi.org/10.1103/PhysRevMaterials.2.123801>
- [12] L. Shen, J. Zhou, T. Yang, M. Yang, Y. P. Feng, High-throughput computational discovery and intelligent design of two-dimensional functional materials for various applications, *Acc. Mater. Research* 3 (6) (2022) 572–583. doi:<https://doi.org/10.1021/accountsmr.1c00246>. URL <https://doi.org/10.1021/accountsmr.1c00246>

- [13] H. Abroshan, H. S. Kwak, A. Chandrasekaran, A. K. Chew, A. Fonari, M. D. Halls, High-throughput screening of hole transport materials for quantum dot light-emitting diodes, *Chem. Mater.* 35 (13) (2023) 5059–5070. doi:<https://doi.org/10.1021/acs.chemmater.3c00561>.
URL <https://doi.org/10.1021/acs.chemmater.3c00561>
- [14] M. H. Mobarak, M. A. Mimona, M. A. Islam, N. Hossain, F. T. Zohura, I. Imtiaz, M. I. H. Rimon, Scope of machine learning in materials research—A review, *Appl. Surf. Sci. Adv.* 18 (2023) 100523. doi:<https://doi.org/10.1016/j.apsadv.2023.100523>.
URL <https://doi.org/10.1016/j.apsadv.2023.100523>
- [15] K. Li, B. DeCost, K. Choudhary, M. Greenwood, J. Hattrick-Simpers, A critical examination of robustness and generalizability of machine learning prediction of materials properties, *npj Comput. Mater.* 9 (1) (2023) 55. doi:<https://doi.org/10.1038/s41524-023-01012-9>.
URL <https://doi.org/10.1038/s41524-023-01012-9>
- [16] H. Wang, K. Li, S. Ramsay, Y. Fehlis, E. Kim, J. Hattrick-Simpers, Evaluating the performance and robustness of LLMs in materials science Q&A and property predictions, *Digital Discovery* 4 (2025) 1612–1624. doi:<https://doi.org/10.1039/D5DD00090D>.
URL <https://doi.org/10.1039/D5DD00090D>
- [17] A. P. Bartók, R. Kondor, G. Csányi, On representing chemical environments, *Phys. Rev. B* 87 (18) (2013) 184115. doi:<https://doi.org/10.1103/PhysRevB.87.184115>.
URL <https://doi.org/10.1103/PhysRevB.87.184115>
- [18] J. Behler, Atom-centered symmetry functions for constructing high-dimensional neural network potentials, *J. Chem. Phys.* 134 (7) (2011). doi:<https://doi.org/10.1063/1.3553717>.
URL <https://doi.org/10.1063/1.3553717>
- [19] M. Rupp, A. Tkatchenko, K.-R. Müller, O. A. Von Lilienfeld, Fast and accurate modeling of molecular atomization energies with machine learning, *Phys. Rev. Lett.* 108 (5) (2012) 058301. doi:<https://doi.org/10.1103/PhysRevLett.108.058301>.
URL <https://doi.org/10.1103/PhysRevLett.108.058301>

- [20] F. Faber, A. Lindmaa, O. A. Von Lilienfeld, R. Armiento, Crystal structure representations for machine learning models of formation energies, *Int. J. Quantum Chem.* 115 (16) (2015) 1094–1101. doi:<https://doi.org/10.1002/qua.24917>. URL <https://doi.org/10.1002/qua.24917>
- [21] K. Hansen, F. Biegler, R. Ramakrishnan, W. Pronobis, O. A. Von Lilienfeld, K.-R. Muller, A. Tkatchenko, Machine learning predictions of molecular properties: Accurate many-body potentials and nonlocality in chemical space, *J. Phys. Chem. Lett.* 6 (12) (2015) 2326–2331. doi:<https://doi.org/10.1021/acs.jpcllett.5b00831>. URL <https://doi.org/10.1021/acs.jpcllett.5b00831>
- [22] A. Chadha, Y. Andreopoulos, Voronoi-based compact image descriptors: Efficient region-of-interest retrieval with VLAD and deep-learning-based descriptors, *IEEE Trans. Multimed.* 19 (7) (2017) 1596–1608. doi:<https://doi.org/10.1109/TMM.2017.2673415>. URL <https://doi.org/10.1109/TMM.2017.2673415>
- [23] H. Huo, M. Rupp, Unified representation of molecules and crystals for machine learning, *Mach. Learn.: Sci. Technol.* 3 (4) (2022) 045017. doi:<https://doi.org/10.1088/2632-2153/aca005>. URL <https://doi.org/10.1088/2632-2153/aca005>
- [24] A. Wang, G. C. Sosso, Graph-based descriptors for condensed matter, *Phys. Rev. E* 111 (6) (2025) 064302. doi:<https://doi.org/10.1103/PhysRevE.111.064302>. URL <https://doi.org/10.1103/PhysRevE.111.064302>
- [25] J. Gilmer, S. S. Schoenholz, P. F. Riley, O. Vinyals, G. E. Dahl, Neural message passing for quantum chemistry, in: D. Precup, Y. W. Teh (Eds.), *Proceedings of the 34th International Conference on Machine Learning*, Vol. 70 of *Proceedings of Machine Learning Research*, PMLR, 2017, pp. 1263–1272. URL <https://proceedings.mlr.press/v70/gilmer17a.html>
- [26] L. Ward, A. Dunn, A. Faghaninia, N. E. Zimmermann, S. Bajaj, Q. Wang, J. Montoya, J. Chen, K. Bystrom, M. Dylla, et al., Matminer: An open source toolkit for materials data mining, *Comput. Mater. Sci.*

- 152 (2018) 60–69. doi:<https://doi.org/10.1016/j.commatsci.2018.05.018>.
URL <https://doi.org/10.1016/j.commatsci.2018.05.018>
- [27] V. M. Pereira, J. Lopes dos Santos, A. Castro Neto, Modeling disorder in graphene, *Phys. Rev. B* 77 (11) (2008) 115109. doi:<https://doi.org/10.1103/PhysRevB.77.115109>.
URL <https://doi.org/10.1103/PhysRevB.77.115109>
- [28] J. Hong, Z. Hu, M. Probert, K. Li, D. Lv, X. Yang, L. Gu, N. Mao, Q. Feng, L. Xie, et al., Exploring atomic defects in molybdenum disulphide monolayers, *Nat. Commun.* 6 (1) (2015) 6293. doi:<https://doi.org/10.1038/ncomms7293>.
URL <https://doi.org/10.1038/ncomms7293>
- [29] D. Thomas, Y. Asiri, N. Drummond, Point defect formation energies in graphene from diffusion quantum monte carlo and density functional theory, *Phys. Rev. B* 105 (18) (2022) 184114. doi:<https://doi.org/10.1103/PhysRevB.105.184114>.
URL <https://doi.org/10.1103/PhysRevB.105.184114>
- [30] A. Kirchhoff, T. Deilmann, P. Krüger, M. Rohlfing, Electronic and optical properties of a hexagonal boron nitride monolayer in its pristine form and with point defects from first principles, *Phys. Rev. B* 106 (4) (2022) 045118. doi:<https://doi.org/10.1103/PhysRevB.106.045118>.
URL <https://doi.org/10.1103/PhysRevB.106.045118>
- [31] R. M. Tromer, Dynamic collision fingerprints (DCF): Introducing a new descriptor linking lattice interactions to 2D structural data signatures, *J. Chem. Theory Comput.* 21 (16) (2025) 8106–8118. doi:<https://doi.org/10.1021/acs.jctc.5c00856>.
URL <https://doi.org/10.1021/acs.jctc.5c00856>
- [32] P. Drude, Zur elektronentheorie der metalle, *Annalen der Physik* 312 (3) (1902) 687–692. doi:<https://doi.org/10.1002/andp.19003060312>.
URL <https://doi.org/10.1002/andp.19003060312>
- [33] T. Schneider, Classical statistical mechanics of lattice dynamic model systems: transfer integral and molecular-dynamics studies, in: *Statics and Dynamics of Nonlinear Systems: Proceedings of a Workshop at the*

Ettore Majorana Centre, Erice, Italy, 1–11 July, 1983, 1983, pp. 212–241.

- [34] T. M. Hope, Linear regression, in: A. Mechelli, S. Vieira (Eds.), Machine learning, Elsevier, 2020, pp. 67–81. doi:<https://doi.org/10.1016/B978-0-12-815739-8.00004-3>.
URL <https://doi.org/10.1016/B978-0-12-815739-8.00004-3>
- [35] J. R. Quinlan, Induction of decision trees, Machine Learning 1 (1) (1986) 81–106. doi:<https://doi.org/10.1007/BF00116251>.
URL <https://doi.org/10.1007/BF00116251>
- [36] T. Chen, C. Guestrin, XGBoost: A scalable tree boosting system, in: Proceedings of the 22nd acm sigkdd international conference on knowledge discovery and data mining, Association for Computing Machinery, New York, NY, USA, 2016, pp. 785–794. doi:<https://doi.org/10.1145/2939672.293978>.
URL <https://doi.org/10.1145/2939672.293978>
- [37] X. Shi, S. Li, J. Li, T. Ouyang, C. Zhang, C. Tang, C. He, J. Zhong, High-throughput screening of two-dimensional planar sp^2 carbon space associated with a labeled quotient graph, J. Phys. Chem. Lett. 12 (47) (2021) 11511–11519. doi:<https://doi.org/10.1021/acs.jpcllett.1c03193>.
URL <https://doi.org/10.1021/acs.jpcllett.1c03193>
- [38] S. P. Ong, W. D. Richards, A. Jain, G. Hautier, M. Kocher, S. Cholia, D. Gunter, V. L. Chevrier, K. A. Persson, G. Ceder, Python materials genomics (pymatgen): A robust, open-source python library for materials analysis, Comput. Mater. Sci. 68 (2013) 314–319. doi:<https://doi.org/10.1016/j.commatsci.2012.10.028>.
URL <https://doi.org/10.1016/j.commatsci.2012.10.028>